Proceedings of ASME Turbo Expo 2011
GT2011
June 6-10, 2011, Vancouver, British Columbia, Canada

GT2011-46476

ANISOTROPIC CREEP DAMAGE AND ELASTIC DAMAGE OF NOTCHED DIRECTIONALLY SOLIDIFIED MATERIALS

Calvin M. Stewart
Department of Mechanical, Materials, & Aerospace Engineering, University of Central Florida
Orlando, FL USA 32816-2450

Ali P. Gordon
Department of Mechanical, Materials, & Aerospace Engineering, University of Central Florida
Orlando, FL USA 32816-2450

ABSTRACT

Drives to improve gas turbines efficiency have lead to an increase in firing temperatures. This increase in exhaust temperature has a negative impact upon turbine blade life. Both engineers and material scientists have produced methods to improve turbine blade life under these conditions. Cooling holes have become commonplace and use relatively cool gas to create a lower temperature barrier around a turbine blade. These cooling holes creating internal and external surfaces; a common sight of crack initiation. Directionally-solidified (DS) turbine blades have also become commonplace. These turbine blades exhibit a transversely-isotropic grain structure that improves creep strength in a desired direction. To model a component under such conditions, anisotropic constitutive models are required. In this paper, an anisotropic tertiary creep damage constitutive model for transversely-isotropic materials is given. The influence of creep-damage on general linear elasticity (elastic damage) is described by a modified Hooke's compliance tensor. Finite element simulations of a V-notched tensile specimen are conducted to replicate a crack initiation site. A discussion on stress triaxiality, stress redistribution, and damage distribution due to anisotropy is provided.

KEYWORDS: Continuum Damage Mechanics, Elastic Damage, Crack Initiation, Constitutive Modeling, Tranversely-Isotropic

1. INTRODUCTION

Gas turbine blades undergo severe load and environmental conditions that facilitate the evolution of microstructural damage. The high operating temperatures, mechanical stresses, thermal gradients, fuel and air contaminates, and solid particles lead to a number of damage mechanisms. These damage mechanisms include; creep, thermal fatigue, thermomechnical fatigue, corrosion, erosion, oxidation, and foreign object damage [1].

Due to the high heat flux from hot combustor exhaust gases, turbine blade experience high temperatures that significantly reduce component life [2]. To extend the operational lifetime of a turbine airfoils; coating, internal cooling, and film cooling methods have been introduced. Coatings thermally insulate a turbine airfoil from the environment. Both film and internal cooling methods use internal channels within a airfoil to direct cool gas to either the outside surface or inner body. A cooled turbine vane is shown in Figure 1. These internal channels and holes are susceptible to most damage mechanisms and are a common site of crack initiation.

Turbine blades experience a complex state of stress. Centrifugal forces are a result of rotational speeds ranging from zero to hundreds of thousands of rpm depending on application. Distortions in the flow field at the blade surface, rotor dynamics, and shroud tip rub may give rise to dynamic flexural stresses [3]. Stress at the blade root/seat location may give rise to wear. Under cyclic conditions this can lead to flexural, vibratory, and fretting fatigue. Multiaxiality arises from a confluence of geometric and generally orthogonal centrifugal, axial, and tangential aero loading with variable amplitude history.

Advances in manufacturing technology have lead to the common use of the directionally-solidification manufacturing process for turbine blades. This process produces a turbine blade with an anisotropic columnar-grained microstructure. These long (L) columnar grains inhibit intergranular cracking and exhibit enhanced strength, ductility, and operational life compared to a polycrystalline material [4]. While the long columnar grains increase the resilience of the material, the anisotropic microstructure introduces planes of material

 Copyright © 2011 by ASME

weakness which can accelerate crack initiation at stress concentrations such as cooling holes and channels.

The multiaxial state of stress, high temperature, and anisotropic grain microstructure at cooling holes on a turbine blade generate a complex creep condition. A method is needed to determine the creep strain that arises. In this paper, a multiaxial creep damage constitutive model for transversely-isotropic materials developed by the authors is presented. An elastic damage formulation is developed. The geometry of a V-notched specimen is setup in Finite Element Analysis (FEA) software and used to approximate the stress concentration found at a cooling hole. Using the material properties of a directionally-solidified Ni-base superalloy, simulations are performed. The results of FEA are examined and compared to knowledge of material behavior. A detailed discussion on the influence of stress triaxiality and material planes of weakness at the crack initiation site is provided.

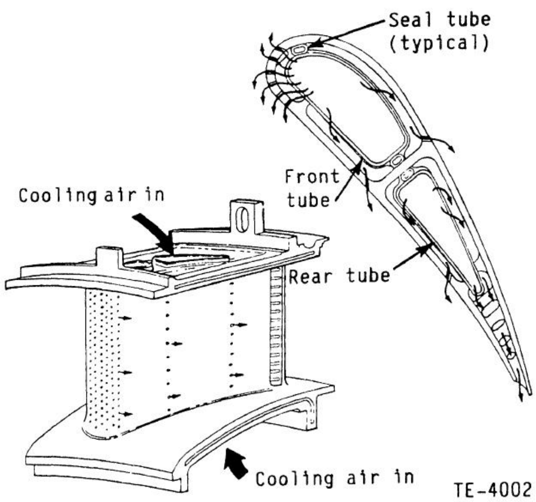

Figure 1 - Cooled Turbine Vane

2. CONSITUTIVE MODEL

1.1. Anisotropic Creep Damage

The constitutive model is based upon the Kachanov-Rabotnov creep damage equations for isotropic materials. Kachanov [5] and Rabotnov [6] proposed equations for the creep rate and damage evolution are as follows

$$\dot{\varepsilon}_{cr} = \frac{d\varepsilon_{cr}}{dt} = A\left(\frac{\bar{\sigma}}{1-\omega}\right)^{n} \tag{1}$$

$$\dot{\omega} = \frac{d\omega}{dt} = \frac{M\bar{\sigma}^{\chi}}{(1-\omega)^{\phi}} \tag{2}$$

where the creep strain rate equates to Norton's power law for secondary creep [7] with constants A and n constants, $\bar{\sigma}$ is equivalent stress, and M, χ, and ϕ are tertiary creep damage constants. Creep damage is considered the reduction-in-area from microcrack and voids. The Kachanov-Rabotnov model has been implemented in a number of forms [8-10]. The secondary creep constants can be found by equating Eq. (1) the minimum creep strain rate. The tertiary creep constants can be found using an analytical technique developed by the authors [11]. Numerical optimization can also been used [12].

A multiaxial extension of the creep rate can be produced using a plastic potential function. A general flow rule with multiaxial stress can be adopted using a plastic potential function such as follows

$$d\varepsilon_{ij,cr} = \frac{d\bar{\varepsilon}}{\bar{\sigma}}\frac{d\psi}{d\sigma_{ij}} \tag{3}$$

where $d\bar{\varepsilon}$ is the equivalent strain increment, $\bar{\sigma}$ is the equivalent stress, and $\psi(\sigma_{ij})$ is a plastic potential function. A number of authors have developed specialized adaptations using this technique [13-15].

Adaptation of this method for anisotropic materials requires the use of Hill's anisotropic equivalent stress as follows

$$\begin{gathered}\sigma_{\mathrm{Hill}} = \sqrt{\mathbf{s}^{T}\mathbf{M}\mathbf{s}} \\ \mathbf{s} = \begin{bmatrix}\sigma_{11} & \sigma_{22} & \sigma_{33} & \sigma_{12} & \sigma_{23} & \sigma_{13}\end{bmatrix}^{\mathrm{T}} \\ \mathbf{M} = \begin{bmatrix} G+H & -H & -G & 0 & 0 & 0 \\ -H & F+H & -F & 0 & 0 & 0 \\ -G & -F & F+G & 0 & 0 & 0 \\ 0 & 0 & 0 & 2N & 0 & 0 \\ 0 & 0 & 0 & 0 & 2L & 0 \\ 0 & 0 & 0 & 0 & 0 & 2M \end{bmatrix}\end{gathered} \tag{4}$$

where $\mathbf{s}$ is the Cauchy stress vector and $\mathbf{M}$ is the Hill compliance tensor consisting of the F, G, H, L, M, and N unitless material constants [16]. This approach allows for three orthogonal planes of symmetry. Adjusting the Hill material constants can decrease the number of symmetric orthogonal planes.

Using the general flow rule Eq. (3) and Hill's anisotropic equivalent stress Eq. (4), a multiaxial creep strain rate for anisotropic materials is defined as follows

$$\dot{\mathbf{e}}^{cr} = A_{aniso}\tilde{\sigma}_{\mathrm{Hill}}{}^{n_{aniso}}\frac{\mathbf{Ms}}{\sigma_{\mathrm{Hill}}} \tag{5}$$

where A_{aniso}, n_{aniso} are the anisotropic secondary creep material constants, $\mathbf{M}$ is the Hill compliance tensor, $\mathbf{s}$ is the Cauchy stress vector, and $\tilde{\sigma}_{\mathrm{Hill}}(\boldsymbol{\omega})$ is the effective Hill's equivalent stress a function of $\boldsymbol{\omega}$, the damage tensor. Using the Hill equivalent stress as a basis for multiaxial extension provides a

Copyright © 2011 by ASME

number of positive attributes. Hill's analogy depends on the deviatoric stresses; therefore, the new approach maintains inelastic incompressibility. The compliance tensor, **M** imparts coordinate system dependence allowing for up to three orthogonal planes of symmetry.

Difficultly arises when attempting to produce a multiaxial damage evolution equation. The Kachanov-Rabotnov damage evolution, Eq. (2), has current damage, ω, in the denominator and to a power of ϕ the material constant. Other authors have avoided this issue by eliminating the constant in the denominator [17]. In this paper, the additional constant is not ignored and thus necessitates division of the multiaxial form into two parts as follows

$$\mathbf{b} = M_{aniso}\sigma_{Hillb}^{\chi_{aniso}} \frac{\mathbf{M}_b \mathbf{s}}{\sigma_{Hillb}} \qquad \boldsymbol{\lambda} = \phi_{aniso} \frac{\mathbf{M}_\lambda \mathbf{s}}{\sigma_{Hill\lambda}} \tag{6}$$

where M_{aniso}, χ_{aniso}, and ϕ_{aniso} are anisotropic tertiary creep damage constants and **s** is the Cauchy stress vector, and $\mathbf{M}_\text{b}$ and $\mathbf{M}_\lambda$, are unique Hill compliance tensors of the same form as Eq. (4) respectively. The independent *F*, *G*, *H*, *L*, *M*, and *N* constants for each Hill compliance tensor can be found in a similar manor to that outlined in a previous paper by the authors [15]. The multiaxial damage evolution for anisotropic materials comes together as

$$\dot{\omega}_i = \frac{|\mathrm{b}_i|}{(1-\omega_i)^{|\lambda_i|}}. \tag{7}$$

where $\dot{\boldsymbol{\omega}}$ is the damage evolution vector and $\boldsymbol{\omega}$ is the damage vector.

Rabotnov [18] proposed an effective stress tensor where the Cauchy stress vector **s**, and a fourth order damage applied tensor, $\boldsymbol{\Omega}$, produce a symmetric tensor as follows

$$\tilde{\mathbf{s}} = \boldsymbol{\Omega}(\boldsymbol{\omega}) \cdot \mathbf{s} \tag{8}$$

where the damage applied tensor is a function of damage. Extending this concept for the Kachanov-Rabotnov damage evolution, Eq. (2), effective stress leads to the following

$$\tilde{\mathbf{s}} = (\mathbf{I}-\mathbf{D})^{-1}\mathbf{s}, \quad \mathbf{D} = \mathrm{diag}(\omega_1, \omega_2, \ldots, \omega_n)$$
$$\mathbf{D} = \begin{bmatrix} \omega_1 & 0 & 0 & 0 \\ 0 & \omega_2 & 0 & 0 \\ 0 & 0 & \ddots & \vdots \\ 0 & 0 & \cdots & \omega_n \end{bmatrix} \tag{9}$$

where $\boldsymbol{\omega}$ is the damage vector and **I** and **D** represent a fourth rank identity tensor and damage tensor respectively.

1.2. Elastic Damage

The growth of damage within a material not only influences creep behavior but elasticity as well. As damage approaches critical, the number of defects increases. Defects reduce the load carrying capability of a material; therefore, stiffness is reduced (compliance increased). This necessitates the introduction of elastic damage. General linear elasticity can be described by the Hooke's law as

$$\begin{aligned} \mathbf{s} &= \mathbf{Ce} \\ \mathbf{e} &= \mathbf{Ss} \end{aligned} \tag{10}$$

where **s** and **e** are the Cauchy stress and strain tensors and **C** and **S** are the stiffness and compliance tensors respectively.

In 1D isotropic elasticity, elastic damage is most often introduced through a damaged elastic moduli, $\bar{E}$, as follows

$$\bar{E} = E(1-\omega) \tag{11}$$

where *E*, is Young's Modulus, and ω is the isotropic damage. In 2D isotropic elasticity, the following can be used

$$\begin{aligned} \bar{E} &= E(1-\omega_1) \\ \bar{\nu}_{12} &= \nu_{12}\sqrt{1-\omega_1}\big/\sqrt{1-\omega_2} \\ \bar{G} &= G(\bar{E}/E)(\nu/\bar{\nu}) \end{aligned} \tag{12}$$

where $\bar{\nu}_{12}$, ν_{12}, $\bar{G}$, and G are the damaged and undamaged Poisson's ratio and Shear moduli.

Transversely-isotropic materials have two planes of symmetry and require 5 independent elasticity constants. Using a similar approach to the above, a damaged transversely-isotropic compliance tensor is defined in Eq. (13) where the Young's moduli, Poisson's ratios, and shear modulus are E_p, E_z, ν_p, ν_{zp}, ν_{pz}, and G_{zp} respectively. The damaged compliance tensor, $\bar{\mathbf{S}}$, can be used to describe the elastic damage of a transversely-isotropic material.

3. IMPLEMENTATION

The constitutive model is implemented into the general-purpose finite element analysis (FEA) software, ANSYS; however, the approach can be applied in other commercial FEA software. A USERMAT3D user-programmable feature

Table 1 - Nominal chemical composition (wt%) of DS GTD-111 superalloy [20]

Element	Cr	Co	Al	Ti	W	Mo	Ta	C	Zr	B	Fe	Si	Mn	Cu	P	S	Ni
Min	13.7	9.0	2.8	4.7	3.5	1.4	2.5	0.08	0.005	-	-	-	-	-	-	-	Bal.
Max	14.3	10.0	3.2	5.1	4.1	1.7	3.1	0.12	0.040	0.020	0.35	0.3	0.1	0.1	0.015	0.005	Bal.

Copyright © 2011 by ASME

$$
\bar{\mathbf{S}} = \begin{bmatrix}
\frac{1}{E_p\left(1-\omega_1\right)} & -\frac{\nu_p}{E_p\sqrt{1-\omega_1}\sqrt{1-\omega_2}} & -\frac{\nu_{zp}}{E_z\sqrt{1-\omega_1}\sqrt{1-\omega_3}} & 0 & 0 & 0 \\
 & \frac{1}{E_p\left(1-\omega_2\right)} & -\frac{\nu_{zp}}{E_z\sqrt{1-\omega_2}\sqrt{1-\omega_3}} & 0 & 0 & 0 \\
 & & \frac{1}{E_z\left(1-\omega_3\right)} & 0 & 0 & 0 \\
 & & & \frac{1+\nu_p}{E_p\left(1-\omega_{12}\right)} & 0 & 0 \\
 & & & & \frac{1}{2G_{zp}\left(1-\omega_{23}\right)} & 0 \\
 sym & & & & & \frac{1}{2G_{zp}\left(1-\omega_{13}\right)}
\end{bmatrix} \qquad (13)
$$

(UPF) is coded in FORTRAN. In USERMAT3D, the strain increment, strain, and stress vectors are provided. An updated stress vector must be output. Both the anisotropic tertiary creep damage constitutive model and Modified Hooke's law for transversely-isotropic materials are written into USERMAT3D.

An input deck using the ANSYS parametric design language (APDL) has been created. In the input deck a 3D V-notched specimen quarter model geometry is generated. Appropriate displacement constraints are applied. Constants load and temperature boundary conditions are set. The input deck is flexible such that geometric dimensions and boundary conditions can be parametrically exercised.

The subject material is Directionally-Solidified (DS) GTD-111, a dual phase γ- γ' Ni-base superalloy. The material consists of a FCC austentic nickel γ matrix with a γ' precipitated phase of L12 structured nickel-aluminde (Ni3Al) with a bimodal distribution. The chemical composition is provided in Table 1. The subject material DS GTD-111 is based upon Rene' 80 and has been used as a 1st through 3rd row turbine blade material. It exhibits a columnar-grained microstructure. The long orientation is referred to as L and the two transverse orientations are T. Creep deformation and rupture experiments were conducted on un-notched L, 45°, and T-oriented specimen of DS GTD-111 according to an ASTM standard E-139 [21] at 871°C. From these experiments the constitutive model material properties were determined. The A_{aniso} and n_{aniso} secondary creep constants are 5.764 x 10^{-21} $MPa^{-n_{aniso}}hr^{-1}$ and 6.507 respectively. The M_{aniso}, χ_{aniso}, and ϕ_{aniso} tertiary creep damage constants are 131.0 x 10^{-11} $MPa^{-\chi}hr^{-1}$, 2.054, and 9.698 respectively. The constants of the Hill compliance tensors listed in Table 2.

Table 2 - Hill's Compliance tensor constants for DS GTD-111

Tensor	*F*	*G*	*H*	*L*	*M*	*N*
M	0.5	0.5	0.387	1.641	1.641	1.273
$\mathbf{M}_b$	0.5	0.5	0.643	1.051	1.051	1.785
$\mathbf{M}_\lambda$	0.5	0.5	-5.08E-3	9.071	9.071	0.490

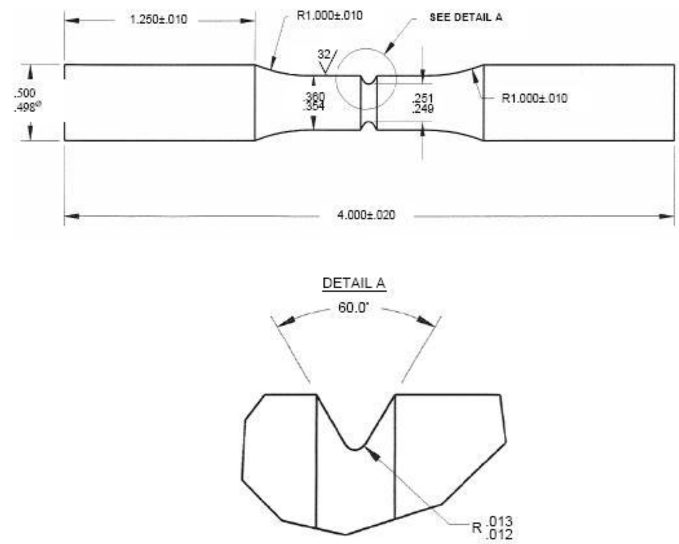

Figure 2 - Notched Specimen Geometry (units in inches)

The V-notched geometry was adopted from previous research and is shown in Figure 2 [19]. The notch geometry follows the ASTM Standard Test method for Sharp-Notch Tension Testing with Cylindrical Specimens [22]. In an effort to provide an accurate FE solution, mesh sensitivity is characterized by the value of the elastic stress concentration factor. In this study, the elastic stress concentration factor, K_t is characterized as

$$K_t = \sigma_{MAX} / \sigma_{NOM} \qquad (14)$$

where the maximum and nominal Hill's equivalent stresses of the 3D FEM are utilized.

In FEM the geometry is separated into near notch, reduced, and grip volumes. Each volume is given a different mesh size with the finest applied to near notch. A series of elastic simulations with elastic damage disabled are conducted to evaluated mesh sizing. A table of the mesh sizes, number of nodes and elements, and the resulting elastic stress concentration factor for an L-oriented specimen is provided in

Copyright © 2011 by ASME

Table 3 - Mesh Sensitivity of L-oriented DS GTD-111 V-notch specimen

	Mesh Size (element edge length, mm)			Number of		Elastic stress concentration factor, K_t		
Mesh	Near Notch	Reduced	Grip	Elements	Nodes	Elem Sol.	Nod Sol.	Error
1	0.5	0.75	1	3424	3975	5.568	5.029	9.68%
2	0.25	0.5	1	6064	6985	7.114	6.961	2.16%
3	0.2	0.4	1	7864	9043	7.659	7.565	1.22%

Table 3. The elastic stress concentration factor increases as mesh size is decreased. The accuracy of a solution can be determined by the error between the element and nodal solutions. It is observed that Mesh 3 holds an error of less than 2%. Mesh 3 was selected for use and is shown in Figure 3.

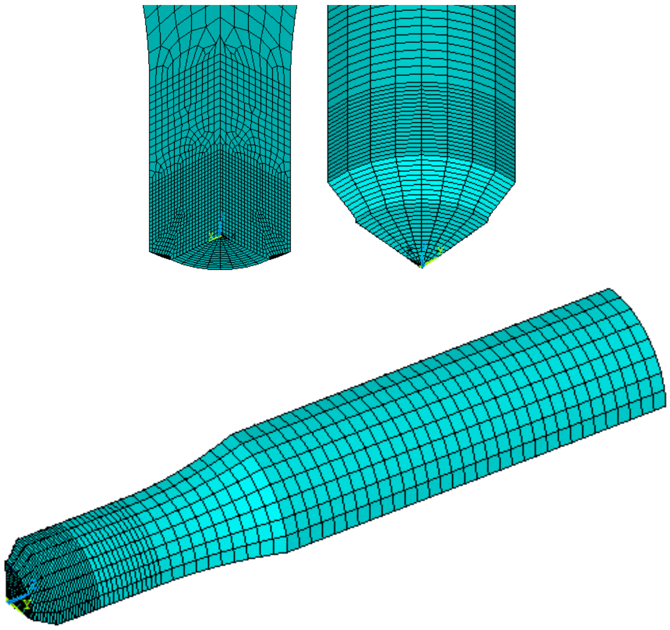

Figure 3 - V-notched FEM Mesh

4. RESULTS & DISCUSSION

The constitutive model has been extensively exercised and validated through comparison with a library of unnotched tensile tests data for DS GTD-111 [23].

A simulation was conducted of an L-oriented DS GTD-111 specimen at 289MPa and 871°C and terminated at 672hrs. An analysis of equivalent stress was performed. When comparing the Von Mises and Hill's equivalent stress it is noticed that the distribution of stress is the same; however, the magnitudes are different. The maximum value of Von Mises stress is 271MPa while Hill's equivalent stress is 281MPa. This is due to dependence on material and load orientation within Hill's equivalent stress. As the subject material is transversely-isotropic, the state of stress is dependent on orientation of the material grain. Therefore, Hill's analogy produces a more accurate measure of equivalent stress for anisotropic materials. The difference between Von Mises and Hill's equivalent stress has a major impact on the stress field at the notch which influences the damage evolution leading to crack initiation. When using Von Mises for anisotropic materials, creep strain is under-predicted and rupture time over-predicted. Often these deficits are corrected using a triaxial stress function relating Von Mises and hydrostatic stress [24]. Instead Hill's equivalent stress should be used as it explicitly accounts for stress-traxiality and anisotropic material behavior.

A depiction of Hill's equivalent stress over time with elastic damage enabled is provided in Figure 4. The quarter model results were expanded to give a full representation of the notched specimen. It is observed that the stress field at the notch changes over time. This is attributed to elastic damage

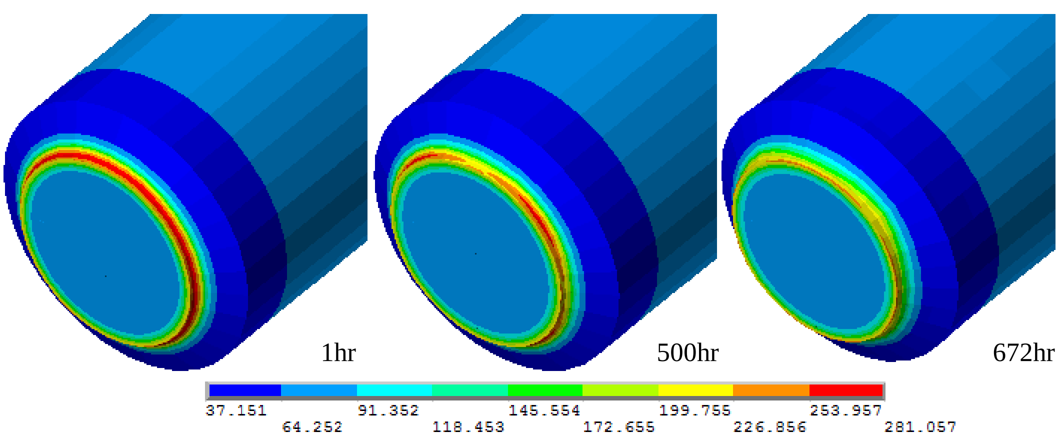

Figure 4 –Redistribution of Hill's equivalent stress, MPa

 Copyright © 2011 by ASME

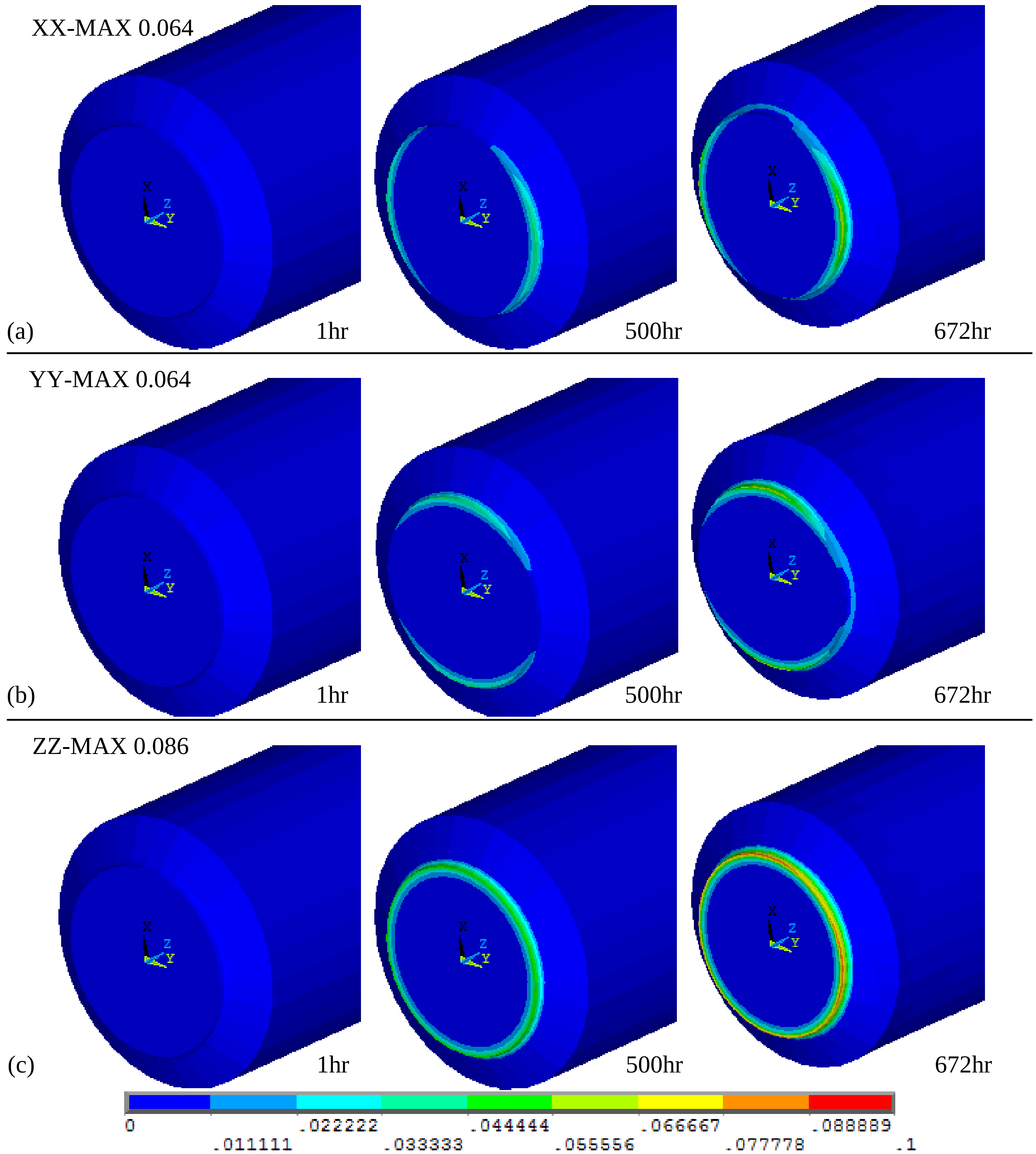

Figure 5 - Normal Damage Evolution (a) XX (b) YY (c) ZZ normal terms

that allows a redistribution of the stress at locations of reduced stiffness. The maximum Hill's equivalent stress is initially located high on the notch. This is due to the shear stress that develops at the notch activating the shear planes of weakness in the material. As shear damage evolves and becomes dominant, the stress is redistributed to a location lower on the notch.

The damage evolution of the normal terms is given in Figure 5. It is observed that damage on each normal evolves based on the oriented material properties Eq. (6), damage history Eq. (7), and reduced stiffness, Eq. (13). The damage on XX and YY normal terms evolve identical as expected of an L-oriented specimen where the long grains are oriented along the ZZ normal. The maximum normal damage occurs in the direction of loading (ZZ) as 0.086. Normal damage is small compared to the shear damage.

The damage evolution of the shear terms is given in Figure 6. Again each shear damage term evolves based on oriented material properties, damage history, and reduced stiffness. It is observed that a majority of damage is found in the shear orientations at the notch, particularly the identical YZ and XZ orientations. Often critical damage, ω_{cr} (the damage at which crack initiation is expected) is estimated at 0.90. The YZ and XZ damage at 672 hrs is found be reach critical damage, therefore crack initiation occurs at the notch due to shear damage. At this point crack propagation would begin. Examining the total damage evolution the simulation is

Copyright © 2011 by ASME

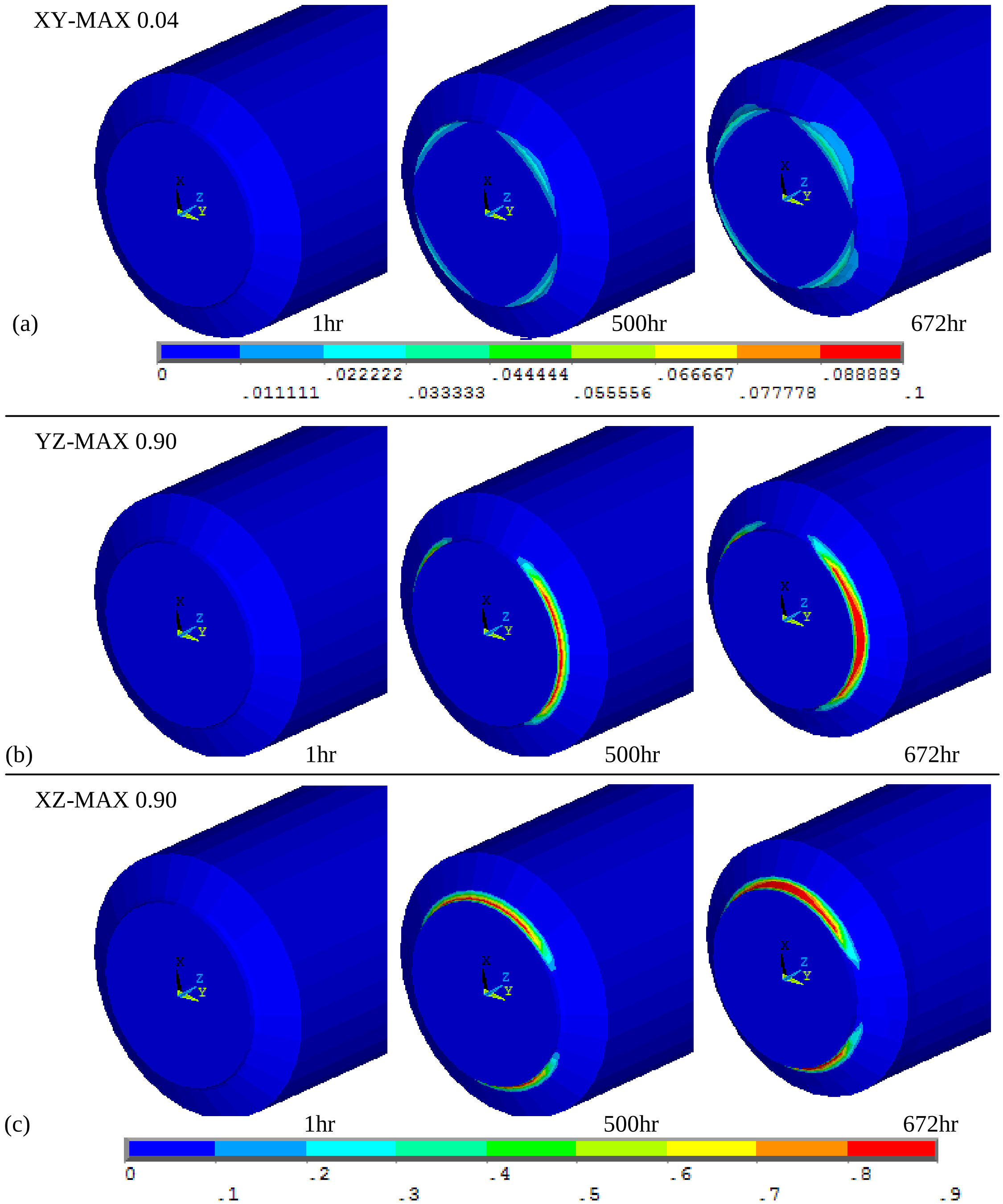

Figure 6 - Shear Damage Evolution (a) XY (b) YZ (c) XZ shear terms

found to correctly model a ductile material. Damage evolves strongly along the slip plane in the direction of the maximum shear stress (the YZ and XZ planes). Crack initiation occurs due to the shear planes of weakness.

5. CONCLUSION

In conclusion, an anisotropic creep damage constitutive model for transversely-isotropic materials has been detailed. An elastic damage model for transversely-isotropic materials has been developed. A 3D V-notched specimen was modeled in finite element software. The appropriate load, boundary conditions, and mesh size were implemented. Material constants were determined such that simulations could be performed. It was shown that Hill's equivalent stress is more accurate for anisotropic materials and eliminates the need for a triaxial stress function. It was demonstrated that elastic damage produces the necessary redistribution of stress observed when a component undergoes damage. It was found that crack initiation of the V-notched specimen is consistent with ductile material behavior. Damage evolves strongly along

Copyright © 2011 by ASME

the slip plane in the direction of the maximum shear stress. Future work will focus on developing an appropriate critical damage criterion for anisotropic materials such that failure is reached based on some critical damage equivalence.

6. ACKNOWLEDGEMENTS

Calvin Stewart is thankful for the support of a Mcknight Doctoral Fellowship through the Florida Education Fund. Ali P. Gordon recognizes the support of the Florida Center for Advanced Aero-Propulsion (FCAAP).

REFERENCES

[1] Mazur, Z., Luna-Ramirez, A., Juarez-Islas, J. A., and Campos-Amezcua, A., 2005, "Failure Analysis of a Gas Turbine Blade made of Inconel 738LC Alloy," *Engineering Failure Analysis*, **12**(3), pp 474-486.

[2] Noot, M., 1997, "Numerical Analysis of Turbine Blade Cooling Ducts", Ph.D. Thesis, Eindhoven University of Technology, Eindhoven.

[3] Stewart, C. M., and Gordon, A. P., 2010, "A Creep Rupture Time Model for Anisotropic Creep-Damage of Transversely-Isotropic Materials," *ASME TURBOEXPO 2010*, GT2010-22532, Glasglow, UK, June 14-18th.

[4] National Research Council (U.S.) Committee on Materials for Large Land-Based Gas Turbines, 1986, *Materials for large land-based gas turbines*, National Academy Press.

[5] Kachanov, L. M., 1967, *The Theory of Creep*, National Lending Library for Science and Technology, Boston Spa, England, Chaps. IX, X.

[6] Rabotnov, Y. N., 1969, *Creep Problems in Structural Members*, North Holland, Amsterdam.

[7] Norton, F. H., 1929, *The creep of steel at high temperatures*, McGraw-Hill, London.

[8] Stewart C. M., and Gordon A. P., (2009), "Modeling the Temperature Dependence of Tertiary Creep Damage of a Ni-base Alloy," *Journal of Pressure Vessel Technology*, **131**(5), pp.1-11.

[9] Karaivanov, V. G., Mazzotta, D. W., Chyu M. K., and Slaughter W. S., 2008, "Three-Dimensional Modeling of Creep Damage in Airfoils for Advanced Turbine Systems," *TURBOEXPO 2008*, GT2008-51278, Berlin, Germany, June 9-13th.

[10] Kowalewksi, Z. L., Hayhurst, D. R., and Dyson B. F., 1994, "Mechanisms-Based Creep Constitutive Equations For an Aluminium Alloy," *Journal of Strain Analysis*, **29**(4), pp. 309-316.

[11] Stewart, C. M., and Gordon, A. P., 2010, "Analytical Method to Determine the Tertiary Creep Damage Constants of the Kachanov-Rabotnov Constitutive Model," *ASME International Mechanical Engineering Congress & Exposition 2010*, IMECE2010-39153, Vancouver, British Columbia, Nov 12-18th.

[12] Stewart C. M., Gordon A. P., Hogan, E. A., and Saxena, A., 2010, "Characterization of the Creep Deformation and Rupture Behavior of DS GTD-111 using the Kachanov-Rabotnov Constitutive Model," *Journal of Engineering Materials and Technology* (Awaiting Publication).

[13] Altenbach, J., Altenbach, H., and Naumenko, K., 2004, "Edge Effects in Moderately Think Plates under Creep-Damage Conditions," *Technische Mechanik*, **24**(3-4), pp. 254-263.

[14] Hyde, T. D., Jones, I.A., Peravali, S., Sun, W., Wang, J.G., and Leen S. B., 2005, "Anisotropic Creep Behavior of Bridgman Notch Specimens," *Proceedings of the Institution of Mechanical Engineers, Part L: Journal of Materials: Design and Applications*, **219**(3), pp. 163-175.

[15] Stewart, C. M., and Gordon, A. P., 2010, "Modeling the Tertiary Creep Damage Behavior of a Transversely-Isotropic Material under Multiaxial and Periodic Loading Conditions," *ASME Pressure Vessel and Piping Conference 2010*, PVP2010-25041, Bellevue, Washington, July 18-22nd.

[16] Hill, R., 1950, *The Mathematical Theory of Plasticity*, Oxford University Press, New York.

[17] Peravali, S., Hyde, T. H., Cliffe, K. A., and Leen, S. B., 2009, "An Anisotropic Creep Damage Model for Anisotropic Weld Metal," *Journal of Pressure Vessel Technology*, **131**(2), pp 1-8.

[18] Rabotnov, Y., 1968, "Creep Rupture," *Applied Mechanics Conference*, Stanford University, Palo Alto, pp. 342-349.

[19] Kupkovits, R. A., 2008, "Thermomechanical Fatigue Behavior of the Directionally-Solidified Nickel-Base Superalloy CM247LC", M.S. Thesis, Georgia Institute of Technology, Atlanta, GA.

[20] Schilke P. W., Foster A. D., Pepe J. J., and Beltran A. M., 1992, "Advanced Materials Propel Progress in Land-Based Gas Turbines," *Advanced Materials and Processes*, **141**(4), pp. 22-30.

[21] ASTM E-139, "Standard Test Methods for Conducting Creep, Creep-Rupture, and Stress Rupture Tests of Metallic Materials", ASTM E-139 No. 03.01, West Conshohocken, PA.

[22] ASTM, "ASTM Standard Test Method for Sharp-Notch Tension Testing with Cylindrical Specimens", ASTM E602-03, West Conshohocken, PA.

[23] Stewart, C. M., Gordon, A. P., and Ma, Y. W., 2011, "An Improved Anisotropic Tertiary Creep Damage Formulation," *Journal of Pressure Vessel Technology*, awaiting publication.

[24] Hayhurst, D. R., 1972, "Creep Rupture Under Multi-Axial States Of Stress," *Journal of the Mechanics and Physics of Solids*, **20**(6), pp. 381-382.

 Copyright © 2011 by ASME